Received: 17 January 2022 | Revised: 7 March 2022 | Accepted: 28 March 2022

DOI: 10.1002/jcla.24424

RESEARCH ARTICLE

WILEY

LINC00240 knockdown inhibits nasopharyngeal carcinoma progress by targeting miR-26a-5p

Xing Chen[1] | Guixiang Wu[2] | Jing Qing[1] | Chunlin Li[1] | Xudong Chen[1] | Jian Shen[3]

[1]Department of Otorhinolaryngology, Ningbo First Hospital, Ningbo City, China

[2]Department of Respiratory Medicine, Ningbo Ximen Wangchun Community Health Service Center, Ningbo City, China

[3]Department of Anesthesiology, Jiangsu Province Hospital, Nanjing, China

Correspondence
Jian Shen, Department of Anesthesiology, Jiangsu Province Hospital, No. 300 Guangzhou Road, Gulou District, Nanjing, Jiangsu 222100, China.
Email: shenjian_ssja@163.com

Funding information
This work was supported by Ningbo Natural Fund [Grant Number: 2019C50054]

Abstract

Objective: This study intended to explore the regulatory functions of LINC00240 on nasopharyngeal carcinoma (NPC).

Methods: MiR-26a-5p inhibitor, mimic, and siLINC00240 were transfected into NPC cells. QRT-PCR was employed to assess miR-26a-5p and LINC00240 expressions. The targeting relationship of LINC00240 and miR-26a-5p was analyzed through dual luciferase reporter and RNA immunoprecipitation assay. Cell counting kit-8 assay, colony formation assay, flow cytometry assay, wound healing assay, Transwell assay and in vitro angiogenesis assay were adopted for the evaluation of the effects of LINC00240 or miR-26a-5p and LINC00240 on NPC cells regarding cell proliferation, apoptosis and cycle, migration, invasion, and angiogenesis. EZH2, cell cycle, and epithelial-mesenchymal transition (EMT)-related protein expression was tested through Western blot.

Results: LINC00240 had a high expression in NPC tissues and cell lines. Silenced LINC00240 significantly suppressed the 5-8F and HK1 cell proliferation, invasion, migration, and angiogenesis, but raised cell apoptosis, and cells were blocked in G0/G1 phase. MiR-26a-5p was a target of LINC00240. MiR-26a-5p upregulation suppressed the NPC cell proliferation, migration, invasion, angiogenesis, N-cadherin and EZH2 expression, while it elevated apoptosis and p21, p27 and E-cadherin expressions, whereas miR-26a-5p downregulation performed conversely. LINC00240 knockdown partially offset the effects of miR-26a-5p downregulation on cell proliferation, migration, invasion, angiogenesis, apoptosis, and EZH2.

Conclusion: LINC00240 knockdown restrained cell proliferation, invasion, migration, and angiogenesis, while it advanced apoptosis via miR-26a-5p in NPC by EZH2 inhibition.

KEYWORDS
LINC00240, migration and invasion, MiR-26a-5p, nasopharyngeal carcinoma, proliferation and angiogenesis

1 | INTRODUCTION

Originated from epithelial cells in the nasopharynx, nasopharyngeal carcinoma (NPC) is a malignant tumor belonging to head and neck squamous cell carcinoma (HNSC). [1] There are significant differences in the ethnic and geographical distribution of NPC, with an incidence rate of 20 cases per 100,000 people in China, Singapore, and other eastern countries.[2] NPC, as a disease sensitive to chemotherapy and radiation, is usually treated with intensity-modulated radiation combined with cisplatin.[3] Unfortunately, most patients are resistant to radiotherapy, leading to tumor recurrence or distant metastasis, which ultimately leads to treatment failure.[4] In recent years, at the cellular and molecular level, it has become a research hotspot to explore and conquer cancer to design targeted therapy for tumor growth inhibition by corresponding therapeutic drugs for cancer locus.[5–7] Hence, the understanding of the potential molecular mechanism of NPC progression, especially distant metastasis, may provide new opportunities for the treatment and development of NPC.

Longer than 200 nucleotides, long non-coding RNA (lncRNA) is a class of RNA that is unable to encode proteins.[8] Nowadays, more and more evidences show that lncRNA plays an essential regulatory role in tumorigenesis and development.[9] Recent studies have shown that lncRNA can promote the formation and progress of a variety of tumors, and it can play a role as both oncogene and tumor suppressor gene. Currently, lncRNA has become a popular research issue in the field of tumor.[10 11] LINC00240 is a newly discovered lncRNA in recent years, which is proven to be abnormally modulated in diverse tumor diseases and can regulate the initiation and progression of tumors like gastric cancer, hepatocellular carcinoma, esophageal squamous cell carcinoma, and cervical cancer.[12–15] Nevertheless, there are few reports on the role of LINC00240 in NPC at present.

Studies have shown that lncRNA can work together with microRNA (miR) to regulate the progression of disease.[16] And former researches have revealed that LINC00240, functioning as a competing endogenous RNA (ceRNA), modulates various miRNAs to be implicated in several types of cancers.[12–15] As a member of miRNAs, miR-26a plays a pivotal part in the treatment of a variety of malignant diseases including NPC.[17–20] In this study, miR-26a-5p was predicted as a target of LINC00240 through bioinformatics analysis, so we discuss the functions of LINC00240 and miR-26a-5p on the pathogenesis of NPC to probe into the specific mechanisms involved in it.

2 | MATERIALS AND METHODS

2.1 | Bioinformatics

The differentially expressed LINC00240 and miR-26a-5p between HNSC and normal tissue samples were analyzed through starBase (http://starbase.sysu.edu.cn/) which, in combination with The Cancer Genome Atlas (TCGA) database (https://www.cancer.gov/about-nci/organization/ccg/research/structural-genomics/tcga), was also utilized for the prediction of miRNAs target by LINC00240.

2.2 | Cell culture

Human NPC cell lines (HK1, 5-8F, C666, SUNE1, 6-10B) and nasopharyngeal epithelial cell line (NP69) were purchased from Shanghai institute of biological sciences, Chinese academy of sciences (Shanghai, China), which were cultivated by RPMI-1640 enriched with 10% fetal bovine serum (FBS, Gibco, USA) in a 5% CO_2 atmosphere at 37°C.

2.3 | Transfection

As LINC00240 had a high expression in 5-8F cells and HK1 cells, so 5-8F cells and HK1 cells were selected for a subsequent experimental study on gene inhibition. The medium was placed in a cell dish (6 pore), and 1×10^6 cells in 2 ml cell solution were added to each pore of the cell dish, and the cell dish was incubated in an atmosphere with 5% CO_2 at 37°C until the cells reached 50% fusion. A transdye preparation: 20 pmol of the small interfering LINC00240 (siLINC00240; 5′-UGUUCUUCCUGUAUUUCUGAG-3′, 5′-CAGAAAUACAGGAAGAACAUC-3′, RiboBio), si-negative control (siNC; siN0000002-1-5, RiboBio), miR-26a-5p mimic (miR10000082-1-5, RiboBio), miR-26a-5p inhibitor (miR20000082-1-5, RiboBio), mimic control (miR1N0000001-1-5, RiboBio), inhibitor control (miR2N0000001-1-5, RiboBio) were diluted in Dulbecco's Modified Eagle Medium (50 μl; DMEM, Hyclone). B transdye preparation: Lipo2000 (Invitrogen) 1 μl was diluted in 50 μl DMEM at room temperature for 15 min and then mixed with A transdye. Thereafter, the mixture was added into cells, following which the cell dish was cultivated in an incubator containing 5% CO_2 at 37°C. Twenty-four hours later, the medium was changed and finally the cells were harvested after 72 h.

2.4 | Luciferase activity assay

A pmirGLO dual luciferase vector (Promega) containing the LINC00240 sequence was constructed to obtain wild-type (WT) pmirGLO-LINC00240. The synthesis of LINC00240 mutant (MUT) in the miR-26a-5 binding sequences was made by a kit (Thermo Fisher Scientific), which was then inserted into a vector to establish MUT pmirGLO-LINC00240. The WT pmirGLO-LINC00240 or MUT pmirGLO-LINC00240 was co-transfected with miR-26a-5 mimic or miR-26a-5 inhibitor to 5-8F and HK1 cells using Lipo2000 (Invitrogen). After incubation for 48 h, the luciferase activity was examined through the Dual-Luciferase Reporter Assay system (Promega).

2.5 | RNA immunoprecipitation (RIP)

According to the guidance of the manufacturer, RIP assay was performed with Magna RIP kit (Millipore). Briefly, lysis buffer (Gibco)

containing RNase inhibitor was applied for lysing 5-8F and HK1 cells. Thereafter, protein A/G agarose beads with AGO2 antibody were added to incubate cell lysates, with normal rabbit IgG as NC. Then, the RNAs that were co-precipitated underwent washing, purification, and examination using qRT-PCR.

2.6 | Quantitative real time-polymerase chain reaction (qRT-PCR)

Total mRNA and miRNA were isolated by Trizol™ reagent (15596018, Thermo Fisher Scientific) and a PureLink™ miRNA Isolation Kit (K157001, Thermo Fisher Scientific), with the concentration of RNA measured by Nanodrop (Thermo Fisher Scientific), and then the RNA was diluted to a concentration of 500 ng/μl. The cDNA was acquired through reverse transcription performed using Superscript II first-strand cDNA synthesis system (Invitrogen). Next, cDNA was amplified with SYBR Green (204057, QIAGEN, https://www.qiagen.com/cn/products/) under a condition of pretreatment at 94°C for 2 min as well as 35 cycles including 94°C for 30 s, 63°C for 30 s, and 72°C for 1 min, followed by 7-min chain extension at 72°C. Eventually, it was kept at 4°C. All primer sequences were listed in Table 1. The respective endogenous controls of mRNA and miRNA were GAPDH and U6. The $2^{-\Delta\Delta CT}$ method was utilized for the evaluation of the expressions of qRT-PCR products.[21]

2.7 | Cell counting kit (CCK)-8 assay

The transfected cells were seeded into the 96-well plate, and CCK-8 (96992, Sigma-Aldrich) solution (10 μl) was added to each well for a 4-h incubation. The absorbance was determined at 450 nm by microplate reader (Thermo Scientific).

2.8 | Colony formation assay

The transfected cells were digested by 0.25% trypsin (C0201, Beyotime Biotechnology), and cultivated in 12-well plates at 100 cells per well in an atmosphere of 5% CO_2 for 3 weeks at 37°C, and the medium was replaced every three days. When the number of colonies was in the range of 50–150 fields, cell culture was stopped. After the removal of the medium, the cells were washed by Dulbecco's phosphate-buffered saline (DPBS, D8662, Sigma-Aldrich) and fixed for 15 min using methanol (1 ml; 34860, Sigma-Aldrich). Then cells were stained with giemsa (1 ml; 999D715, Thermo Fisher Scientific) for 30 min.

2.9 | Cell apoptosis assay

Cells at a density of 1×10^6/ml were suspended in the binding buffer (A21009-100 ml, Alpha Applied Bioscience), subsequent to which FITC Annexin V (5 μl; C1062S, Beyotime Biotechnology) and 1 μl propidium iodide (100 μg/ml; ST511, Beyotime Biotechnology) solution and the binding buffer (300 μl) were cultured with the cell suspension for 15 min at room temperature. Finally, a FACS Calibur TM flow cytometry (BD, Franklin Lakes) was adopted for the analysis of results.

2.10 | Cell cycle assay

Trypsinized for 2 min, cell suspension was centrifuged at 4°C for 5 min at 1,000 *g*, and the supernatant was removed. Cell fixation was done by 70% ice ethanol (3 ml) for 48 h. Subsequently, 400 μl propidium iodide solution (50 μg/ml) was applied to stain the cells. The cell cycle test was analyzed through the flow cytometry.

2.11 | Wound healing assay

The transfected cells were inoculated at 5×10^5 per well on a 6-well plate, and then the cells were cultured for 24 h until the cells were well adhered to the wall. A wound scratch was drawn in the 6-well plate by a pipette head. With the cell debris discarded, low serum concentration (1%) was employed to cultivate the cells. Then, photos at 0 and 48 h were captured under an IXplore Pro microscope (magnification: 100×; Olympus) with Image J, version 1.8.0 applied in the measurement of migration distance.

TABLE 1 Primers used in real-time PCR analysis

Gene	Primer sequence	Species
miR–26a-5p	Forward: 5′-AATCCAGGATAGGCTGTCGT-3′ Reverse: 5′-GTATCCAGTGCGTGTCGTGG-3′	Human
LINC00240	Forward:5′-CGATCTCAGGAGAAGCCAG-3′ Reverse: 5′-TGGTTAGCTTGAGCCTCTG-3′	Human
U6	Forward: 5′-TGACTTCCAAGTACCATCGCCA-3′ Reverse: 5′-TTGTAGAGGTAGGTGTGCAGCAT-3′	Human
GAPDH	Forward: 5′-GGTGAAGGTCGGAGTCAACG-3′ Reverse: 5′-CAAAG TTGTCATGGATGTACC-3′	Human

Abbreviations: GAPDH, glyceraldehyde-3-phosphate dehydrogenase; miR, microRNA.

2.12 | Transwell assay

Cells (1×10^6/ml) were suspended in the upper compartment of Transwell (351184, Corning) pre-coated with Matrigel (354433, Becton Dickinson), whereas the lower compartment was filled with a medium supplemented with 10% FBS serum. After 48 h, 0.5% crystal violet (C0121, Beyotime Biotechnology) was used to stain the cells at the bottom of the upper compartment. The observation was made under the microscope (magnification: 200×).

2.13 | In vitro angiogenesis assay

Matrigel (250 μl/well) was added to a 24-well plate and placed in the cell culture box coagulation for 60 min. The cells were digested with 1 ml trypsin. Next, cells were suspended in the medium to a concentration of 2×10^5/ml. With Matrigel solidified, the plate was taken out, following which the cell suspension (500 μl per well) was added. Thereafter, the cells were cultured for 48 h at 37°C with 5% CO_2. The consequences were observed at 100 times the microscope in 5 random fields.

2.14 | Western blot

Lysed in RIPA lysis buffer (C500007, Sangon Biotech), cells were centrifuged at 4°C, 12,830 *g* for 5 min. With the supernatant harvested, the protein concentration was tested by BCA assay (C503021, Sangon Biotech). SDS-PAGE was performed to separate the equal contents of marker (5 μl; PR1910, Solarbio Science & Technology) and protein (45 μg) through a SDS-PAGE preparation kit (C631100, Sangon Biotech), which was then transferred to PVDF membranes (F019533, Sangon Biotech) and blocked in 5% bovine serum albumin (BSA; E661003, Sangon Biotech) for 1 h at room temperature. Subsequently, membranes were cultured with mouse anti-GAPDH (1:1000; ab8245, Abcam), rabbit anti-EZH2 (1:1000; ab191250, Abcam), rabbit anti-p21 (1:1000; ab109520, Abcam), rabbit anti-p27 (1:5000; ab32034, Abcam), mouse anti-E-cadherin (1:1000; #14472, Cell Signaling Technology), and rabbit anti-N-cadherin (1:1000; #13116, Cell Signaling Technology). After overnight at 4°C, membranes were washed with Tris-buffered saline containing Tween 20 (TBST; C520009, Sangon Biotech) and incubated at room temperature for 1 h with the corresponding secondary antibodies against rabbit (1:2000; ab205718, Abcam) and mouse (1:2000; ab205719, Abcam). Finally, ECL luminescence reagent (C510043, Sangon Biotech) was added to visualize the protein in a chemical imaging system (GelView 6000Plus Smart Gel Imaging System; Biolight Biotechnology) and Image J was applied to data analysis.

2.15 | Statistical analysis

Shown as mean ± standard deviation (SD), data were analyzed through Prism 6 (version 6.01, GraphPad Software). Two groups were contrasted using *t*-test. And the comparison among multiple groups was operated by one-way ANOVA with Bonferroni post hoc. The Venn diagram was employed to identify the intersecting genes of targeting miRNAs of LINC00240 predicted by starBase and downregulated miRNAs in HNSC from TCGA database. $p < 0.05$ indicated a statistical significance.

3 | RESULTS

3.1 | LINC00240 was upregulated in NPC and LINC00240 knockdown restrained proliferation while it facilitated apoptosis in NPC cells

As shown in Figure 1A, the analysis of starBase revealed that the expression of LINC00240 was obviously higher in the HNSC tissues than in normal tissues ($p = 1.3 \times 10^{-7}$). Furthermore, the expression of LINC00240 was significantly higher in the NPC cells than in human nasopharyngeal epithelial NP69 cell line ($p < 0.001$, Figure 1B); 5-8F and HK1 cells were transfected with siNC or siLINC00240. The LINC00240 expression was evidently reduced when the LINC00240 was silenced in NPC cells ($p < 0.01$, Figure 1C,D). The CCK-8 results showed that siLINC00240 suppressed cell viability obviously ($p < 0.01$, Figure 1E,F). After silencing LINC00240, both of 5-8F and HK1 cells conspicuously showed a decline in the rate of colony formation ($p < 0.01$, Figure 1G–I), and cell apoptosis rate was distinctly raised in NPC cells ($p < 0.01$, Figure 1J–L).

FIGURE 1 LINC00240 was upregulated in NPC and LINC00240 knockdown restrained proliferation, while it facilitated apoptosis in NPC cells. (A) StarBase was used to analyze the expression of LINC00240 in HNSC and normal tissues. (B) QRT-PCR was used to detect the expression of LINC00240 in human nasopharyngeal epithelial cell line (NP69) and human NPC cell lines (5-8F, SUNE1, C666, 6-10B, and HK1). The GAPDH was the internal reference. (C and D) The transfection efficiency of LINC00240 in 5-8F and HK1 cell lines was detected by qRT-PCR. The GAPDH was the internal reference. (E and F) CCK-8 was used to detect the effect of LINC00240 on the viability of 5-8F and HK1 cells. (G–I) Colony formation assay detects the proliferative ability of 5-8F and HK1 cells. (J–L) Cell apoptosis was detected by flow cytometry assay in 5-8F and HK1 cells. $^{**}p < 0.01$ versus siNC group. All experiments were repeated independently at least three times. Data are presented as mean ± standard deviation. CCK-8, cell counting kit-8; GAPDH, glyceraldehyde-3-phosphate dehydrogenase; HNSC, head and neck squamous cell carcinoma; NPC, nasopharyngeal carcinoma; qRT-PCR, quantitative real-time polymerase chain reaction; siNC, negative control for siRNA

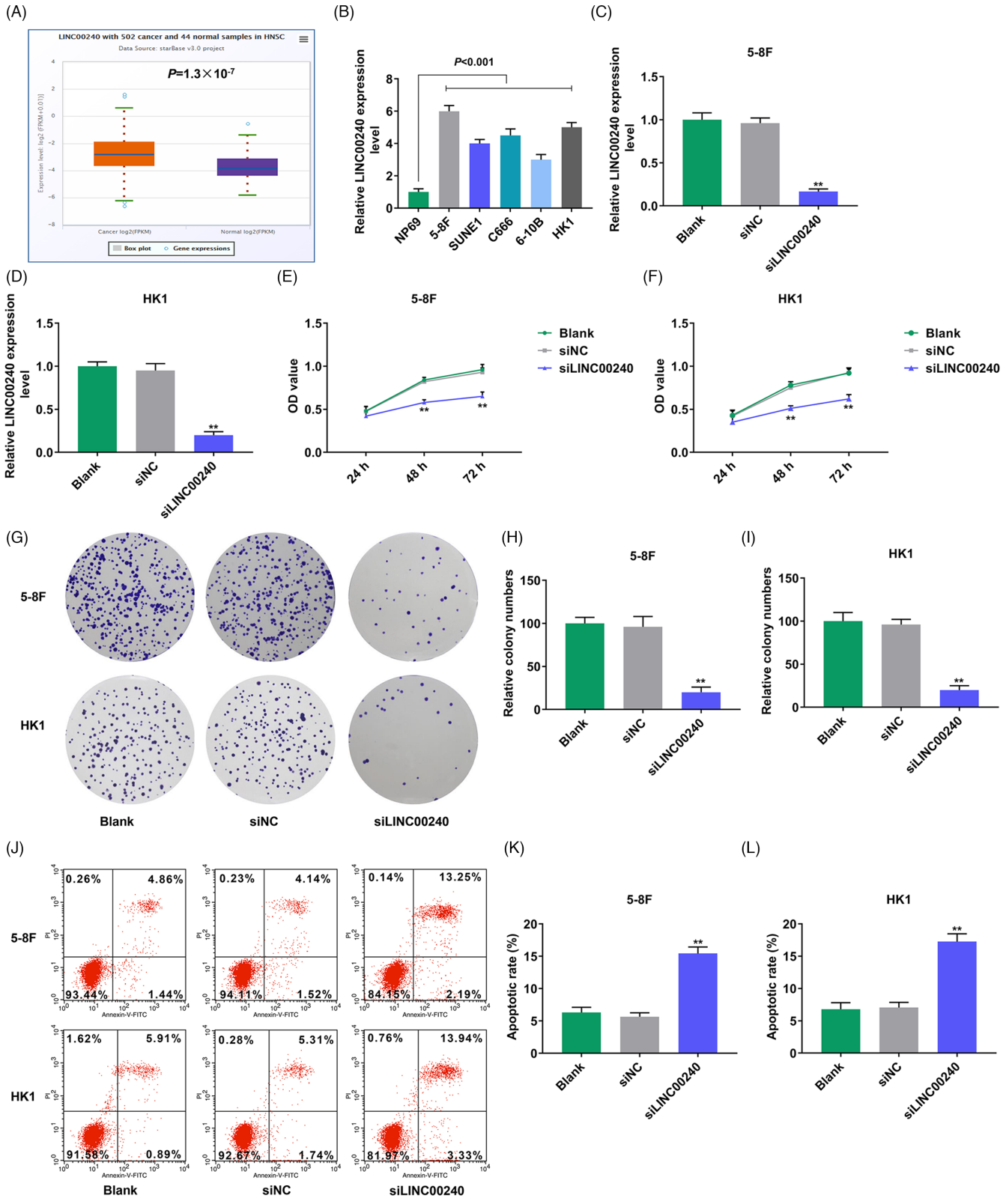

3.2 | LINC00240 knockdown promoted cell cycle block at G0/G1 phase proliferation while it suppressed invasion, migration, and angiogenesis in NPC cells

We found that the number of cells increased in G0/G1 phase after 5-8F and HK1 cells transfected with siLINC00240 ($p < 0.01$, Figure 2A–C). The results of wound healing assay exhibited that siLINC00240 inhibited cell migration ($p < 0.01$, Figure 2D–G). Transwell assay was utilized to detect invasion of 5-8F and HK1 cells, and the consequences displayed that siLINC00240 restrained cell invasion ($p < 0.01$, Figure 3A–C). In addition, the tube length was dramatically decreased after siLINC00240 was transfected into 5-8F and HK1 cells ($p < 0.01$, Figure 3D–F).

3.3 | LINC00240 directly targeted miR-26a-5p

StarBase combined with TCGA indicated that LINC00240 and miR-26a-5p had a targeted correlation (Figure 4A) with the binding sites predicted (Figure 4B). During the dual luciferase reporter assay, 5-8F and HK1 cells with transfection of miR-26a-5p mimic dramatically restrained luciferase activity in the LINC00240-WT group ($p < 0.01$, Figure 4C,D). In addition, RIP assay result showed that the levels of both LINC00240 and miR-26a-5p were greatly enriched by Ago2 antibody compared with control IgG ($p < 0.001$, Figure 4E,F). The miR-26a-5p expression level was significantly increased when LINC00240 was silenced in NPC cells ($p < 0.01$, Figure 4G,H). The level of miR-26a-5p was remarkably decreased in NPC tissue samples ($p = 1.3 \times 10^{-23}$, Figure 4I).

3.4 | The effects of LINC00240 knockdown on proliferation and apoptosis of NPC cells were achieved by upregulating miR-26a-5p

MiR-26a-5p level was upregulated in the mimic group, whereas it was downregulated in the inhibitor group when contrasted with their respective controls, and cells co-transfected with siLINC00240 and miR-26a-5p inhibitor exhibited a higher miR-26a-5p level in comparison with cells with transfection of miR-26a-5p inhibitor alone ($p < 0.01$, Figure 5A,B). The cell viability was obviously elevated when the miR-26a-5p was repressed, but the silence of LINC00240 significantly inhibited the viability of NPC cells relative to inhibited miR-26a-5p ($p < 0.05$, Figure 5C,D). After miR-26a-5p was inhibited in NPC cells, the colony formation ability of cells was notably increased, and declined prominently when LINC00240 was silenced ($p < 0.01$, Figure 5E–G). The cell apoptosis rate was distinctly suppressed by inhibited miR-26a-5p, and silenced LINC00240 obviously reversed the function of miR-26a-5p on apoptosis ($p < 0.05$, Figure 5H–J).

3.5 | The effects of LINC00240 knockdown on NPC cell cycle, invasion, migration, and angiogenesis were achieved by upregulating miR-26a-5p

The number of cells in the G0/G1 phase increased significantly, whereas that in the G2/M phase apparently declined after the elevation of miR-26a-5p ($p < 0.01$, Figure 6A–C). Besides, the inhibited miR-26a-5p obviously enhanced cell migration, and that effect was apparently suppressed by silenced LINC00240 ($p < 0.01$, Figure 6D–G). After miR-26a-5p inhibitor and siLINC00240 were co-transfected into cells, inhibited miR-26a-5p enhanced the cell invasion, and that effect was notably reversed by silenced LINC00240 ($p < 0.01$, Figure 7A–C). Furthermore, inhibited miR-26a-5p accelerated the tube growth, and that effect was rescued evidently by siLINC00240 in NPC cells ($p < 0.05$, Figure 7D–F). In addition, some markers of cell cycle and EMT were detected, and the result showed that miR-26a-5p upregulation promoted the expression of p21, p27, and E-cadherin, inhibited the expression of N-cadherin of NPC cells, while downregulation of miR-26a-5p had the opposite effect ($p < 0.05$, Figures 8A–C). Silencing of LINC00240 partially reversed the effect of downregulation of miR-26a-5p on the expression of p21, p27, E-cadherin, and N-cadherin of NPC cells ($p < 0.05$, Figure 8A–C). Moreover, the Western blot presented that miR-26a-5p upregulation evidently reduced EZH2 protein level of NPC cells, while the downregulation of miR-26a-5p raised that, with the expression of EZH2 in the siLINC00240+inhibitor group prominently lower when contrasted with that in the inhibitor group ($p < 0.01$, Figure 8D–F).

4 | DISCUSSION

Recurrence and high metastasis are bottlenecks in the overall survival of patients with NPC, so this prompts us to look for the cause. LncRNA, which is able to modulate gene expression at transcriptional/post-transcriptional as well as epigenetic levels, is implicated in the silence of X chromosome, transcriptional activation, or interference and other important regulatory processes including the occurrence and progression of diseases.[22,23,24] However, there are few studies on its role in the recurrence of NPC. This study intends to observe the changes in lncRNA expression after differentiation of tumor stem cells, so as to preliminarily reveal the molecular mechanism of NPC recurrence.

As one of the numerous lncRNAs, LINC00240, performed with significantly high level, has been demonstrated to participate in the initiation and advancement of cervical cancer,[15] gastric cancer,[13] hepatocellular carcinoma,[14] and esophageal squamous cell carcinoma,[12] which enable it to be a potential target for cancer treatment. In addition, Bu et al.[14] determined the value of LINC00240 as a possible prognostic biomarker in hepatocellular carcinoma owing to the fact that the high level of LINC00240 notably connects with the shorter survival of hepatocellular carcinoma cases. And the high LINC00240 level has also been identified as a promising predictor for the diagnosis and prognosis of gastric cancer and cervical cancer.[13,15] At present, the mechanism of LINC00240 on NPC is still not clear, so this study discusses its role in NPC. In the present work, we found that LINC00240 had an aberrantly high expression in NPC tissues and cell lines, indicating that LINC00240 might participate in NPC pathogenesis and that LINC00240 probably had a significance in NPC diagnosis and prognosis.

Studies have shown that the downregulation of LINC00240 in hepatocellular carcinoma cells can inhibit cancer cell viability as well as the migratory and invasive abilities.[14] After LINC00240 gene knockout in gastric cancer cells SGC-7901 and BGC-823, cell proliferation, invasion, migration and EMT were significantly restrained.[13] The depletion of LINC00240 can decrease cell invasion, migration, proliferation, and colony formation in cervical cancer, whereas the overexpressed LINC00240 exerted the converse effects.[15] Therefore, we explored the influence of LINC00240 on the NPC cell behaviors, which turned out that the silence of LINC00240

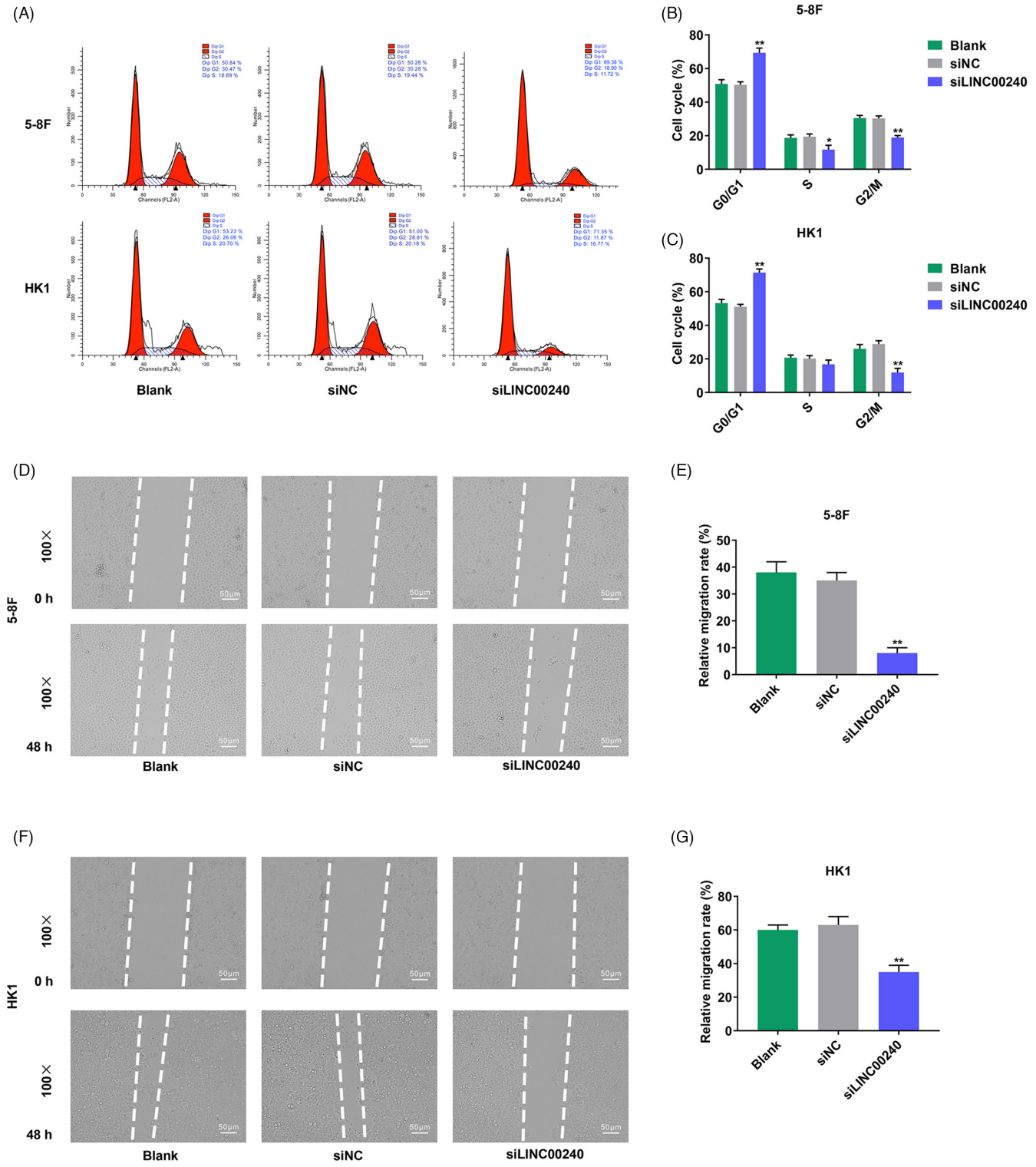

FIGURE 2 LINC00240 knockdown promoted cell cycle arrest at the G0/G1 phase while it suppressed migration in NPC cells. (A–C) Cell cycle was measured by flow cytometry assay in 5-8F and HK1 cells. (D–G) Cell migration was detected by wound healing assay in 5-8F and HK1 cells. $^{*}p < 0.05$, $^{**}p < 0.01$ versus siNC group. All experiments were repeated independently at least three times. Data are presented as mean ± standard deviation. NPC, nasopharyngeal carcinoma; siNC, negative control for siRNA

expression could significantly suppress the NPC cell viability, colony formation, migration, invasion, and angiogenesis, but increase cell apoptosis, and cell block was observed in the G0/G1 phase. This indicated that LINC00240 could regulate the disease course of NPC, and silencing the expression of LINC00240 could inhibit the occurrence and development of NPC.

With the deepening of studies, more and more reports have been obtained on the regulation of lncRNA through binding with other factors to

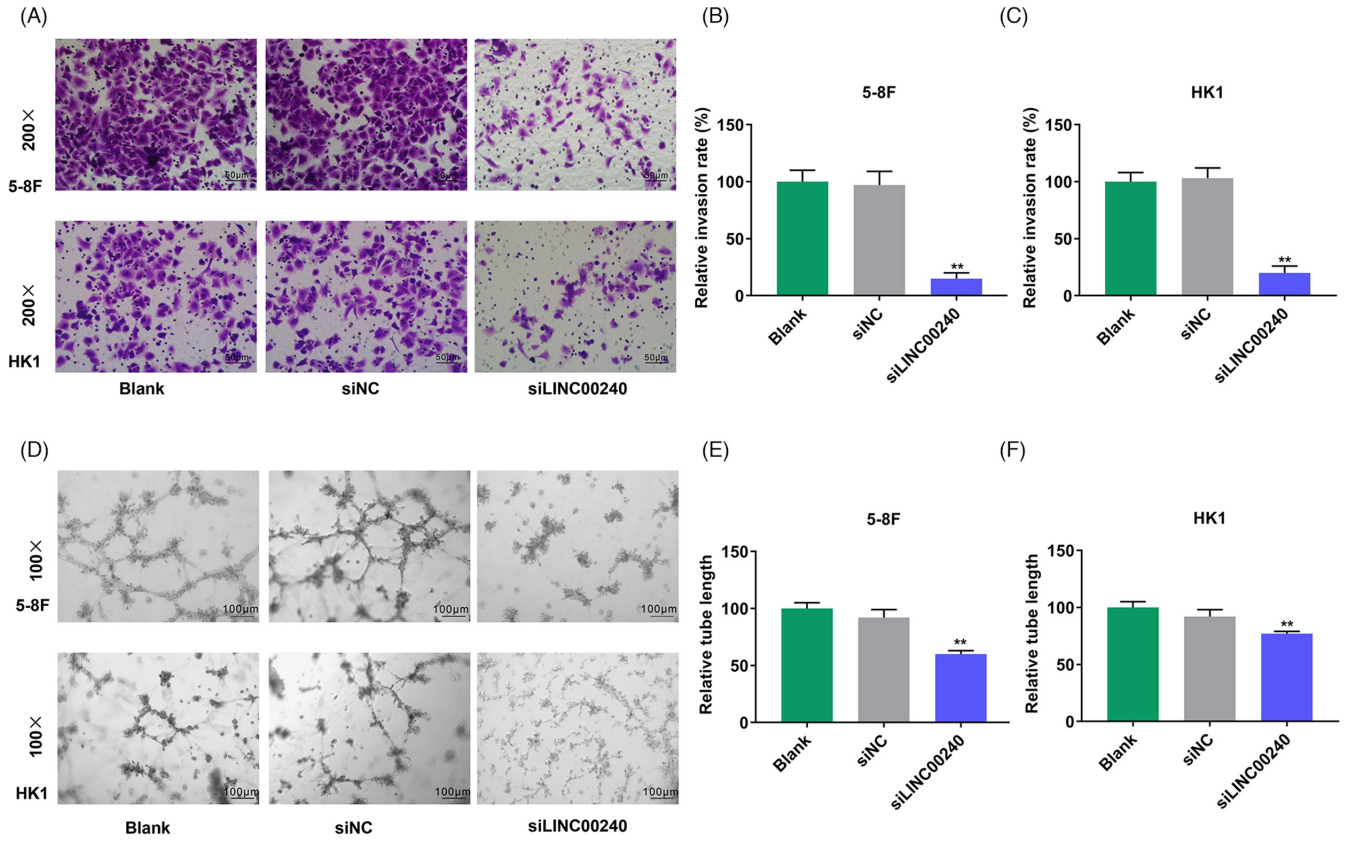

FIGURE 3 LINC00240 knockdown suppressed invasion and angiogenesis in NPC cells. (A–C) Cell invasion was detected by Transwell assay in 5-8F and HK1 cells. (D–F) In vitro angiogenesis experiment was used to detect the angiogenesis. $^{**}p < 0.01$ versus siNC group. All experiments were repeated independently at least three times. Data are presented as mean ± standard deviation. NPC, nasopharyngeal carcinoma; siNC, negative control for siRNA

regulate NPC in the treatment of NPC, such as lncRNA HOTAIR targeting fatty acid synthase and upregulation of its expression in the occurrence of NPC.[25] LncRNA ANRIL enhanced cisplatin-induced NPC cytotoxicity by regulating miR-let-7a.[26] LncRNA ANRIL restrained the proliferation of NPC cells and induced apoptosis by targeting miR-125a.[27]

Similarly, in the regulation of a variety of diseases, LINC00240 can promote or inhibit the progression of diseases by interacting with other factors. Through sponging miR-7-5p, LINC00240 represses non-small-cell lung cancer invasion and migration, while LINC00240 targets miR-4465 to facilitate hepatocellular carcinoma cell proliferation, migration, and invasion by HGF/c-MET pathway.[14,28] Besides, LINC00240 advances gastric cancer tumorigenesis in vitro and in vivo via miR-124-3p/DNMT3B axis, and it is able to promote cervical cancer progression through induction of natural killer T-cell tolerance mediated by miR-124-3p/STAT3/MICA.[13,15] Whether LINC00240 inhibits the disease progression of NPC by regulating a certain gene is still unknown. In this study, we predicted the possible target gene of LINC00240 through starBase and TCGA, and further investigations found that in NPC cells, LINC00240 directly targeted to suppress miR-26a-5p.

MiR-26a-5p plays an important regulatory role in various malignant tumors. Previous reports have shown that the upregulation of miR-26a-5p is able to repress gastric cancer cell proliferation, migration, and invasion via COL10A1, which also restrains the bladder cancer cell proliferation by modulating PDCD10, whereas miR-26a-5p is confirmed to fulfill the oncogenic functions through FAF1 in non-small-cell lung cancer.[29–31] And miR-26a-5p, whose low level predicts a poor

FIGURE 4 LINC00240 directly targeted miR-26a-5p and miR-26a-5p was downregulated in NPC. (A) StarBase combined with TCGA was used to predict the possible target miRNAs of LINC00240. (B) The binding sites between miR-26a-5p and LINC00240 were predicted by starBase. (C and D) Dual-luciferase reporter assay was used to analyze the fluorescence activity of LINC00240 in the upregulation of miR-26a-5p. (E and F) RIP assays were performed using Ago2 antibody or control IgG antibody in 5-8F and HK1 cells, and then qRT-PCR analysis was used to measure the enrichment degrees of LINC00240 and miR-26a-5p in co-precipitated RNA. (G and H) QRT-PCR was used to detect the expression of miR-26a-5p in 5-8F and HK1 cells after transfection of siLINC00240. U6 was the loading control. (I) The differentially expressed miR-26a-5p between HNSC and normal tissue samples was analyzed through starBase. $^{**}p < 0.01$ versus siNC group; $^{\&\&}p < 0.01$ versus mimic control group; $^{\#\#\#}p < 0.001$ versus IgG group. All experiments were repeated independently at least three times. Data are presented as mean ± standard deviation. HNSC, head and neck squamous cell carcinoma; NPC, nasopharyngeal carcinoma; qRT-PCR, quantitative real-time polymerase chain reaction; siLINC00240, small interfering LINC00240; siNC, negative control for siRNA

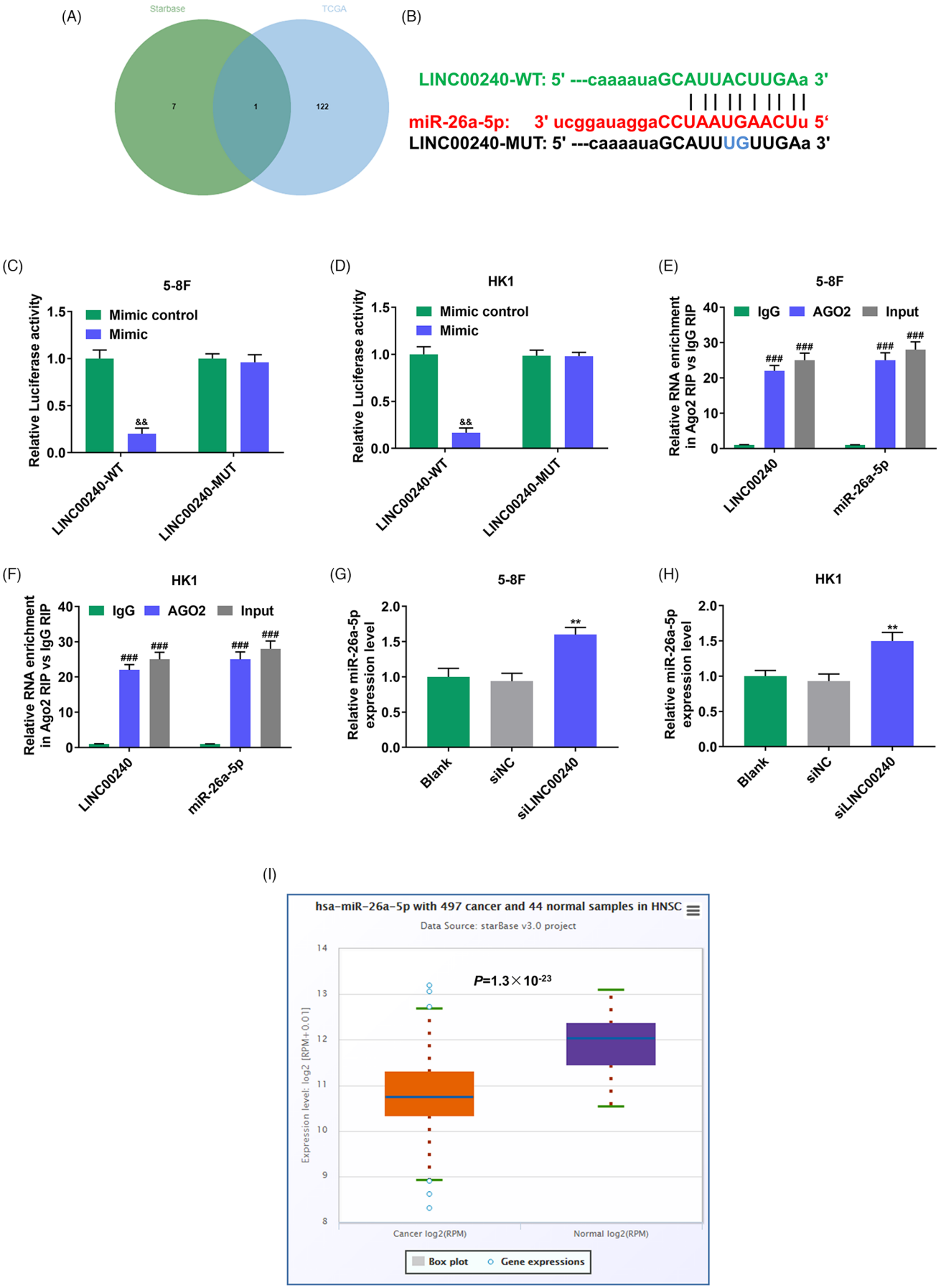
(A)
Starbase
TCGA
7
1
122
(B)
LINC00240-WT: 5' ---caaaauaGCAUUACUUGAa 3'
miR-26a-5p: 3' ucggauaggaCCUAAUGAACUu 5'
LINC00240-MUT: 5' ---caaaauaGCAUUUGUUGAa 3'
(C)
5-8F
Relative Luciferase activity
Mimic control
Mimic
&&
LINC00240-WT
LINC00240-MUT
(D)
HK1
Relative Luciferase activity
Mimic control
Mimic
&&
LINC00240-WT
LINC00240-MUT
(E)
5-8F
Relative RNA enrichment in Ago2 RIP vs IgG RIP
IgG
AGO2
Input
###
LINC00240
miR-26a-5p
(F)
HK1
Relative RNA enrichment in Ago2 RIP vs IgG RIP
IgG
AGO2
Input
###
LINC00240
miR-26a-5p
(G)
5-8F
Relative miR-26a-5p expression level
**
Blank
siNC
siLINC00240
(H)
HK1
Relative miR-26a-5p expression level
**
Blank
siNC
siLINC00240
(I)
hsa-miR-26a-5p with 497 cancer and 44 normal samples in HNSC
Data Source: starBase v3.0 project
P=1.3×10-23
Expression level: log2 [RPM+0.01]
Cancer log2(RPM)
Normal log2(RPM)
Box plot
Gene expressions

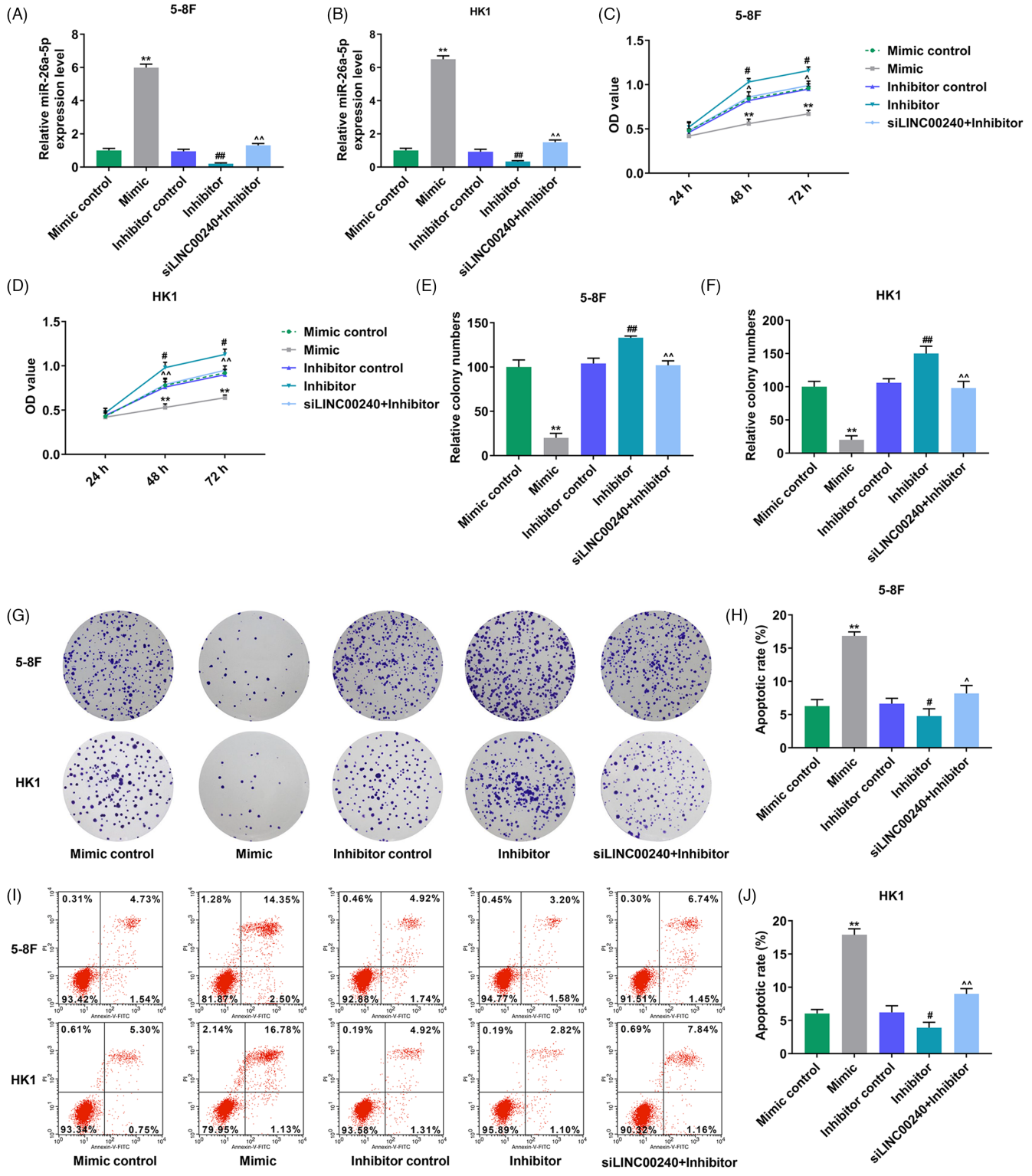

FIGURE 5 The effects of LINC00240 knockdown on proliferation and apoptosis of NPC cells were achieved by upregulating miR-26a-5p. (A–B) The transfection efficiency of miR-26a-5p was detected by qRT-PCR. U6 was the loading control. (C and D) CCK-8 was used to detect the effect of siLINC00240 and miR-26a-5p on viability of 5-8F and HK1 cells. (E–G) Colony formation assay detects the proliferative ability of 5-8F and HK1 cells. (H–J) Cell apoptosis was detected by flow cytometry assay of 5-8F and HK1 cells. $^{**}p < 0.01$ versus mimic control group; $^{\#}p < 0.05$, $^{\#\#}p < 0.01$ versus inhibitor control group; $^{\wedge}p < 0.05$, $^{\wedge\wedge}p < 0.01$ versus inhibitor group. All experiments were repeated independently at least three times. Data are presented as mean ± standard deviation. CCK-8, cell counting kit-8; GAPDH, glyceraldehyde-3-phosphate dehydrogenase; NPC, nasopharyngeal carcinoma; qRT-PCR, quantitative real-time polymerase chain reaction; siLINC00240, small interfering LINC00240

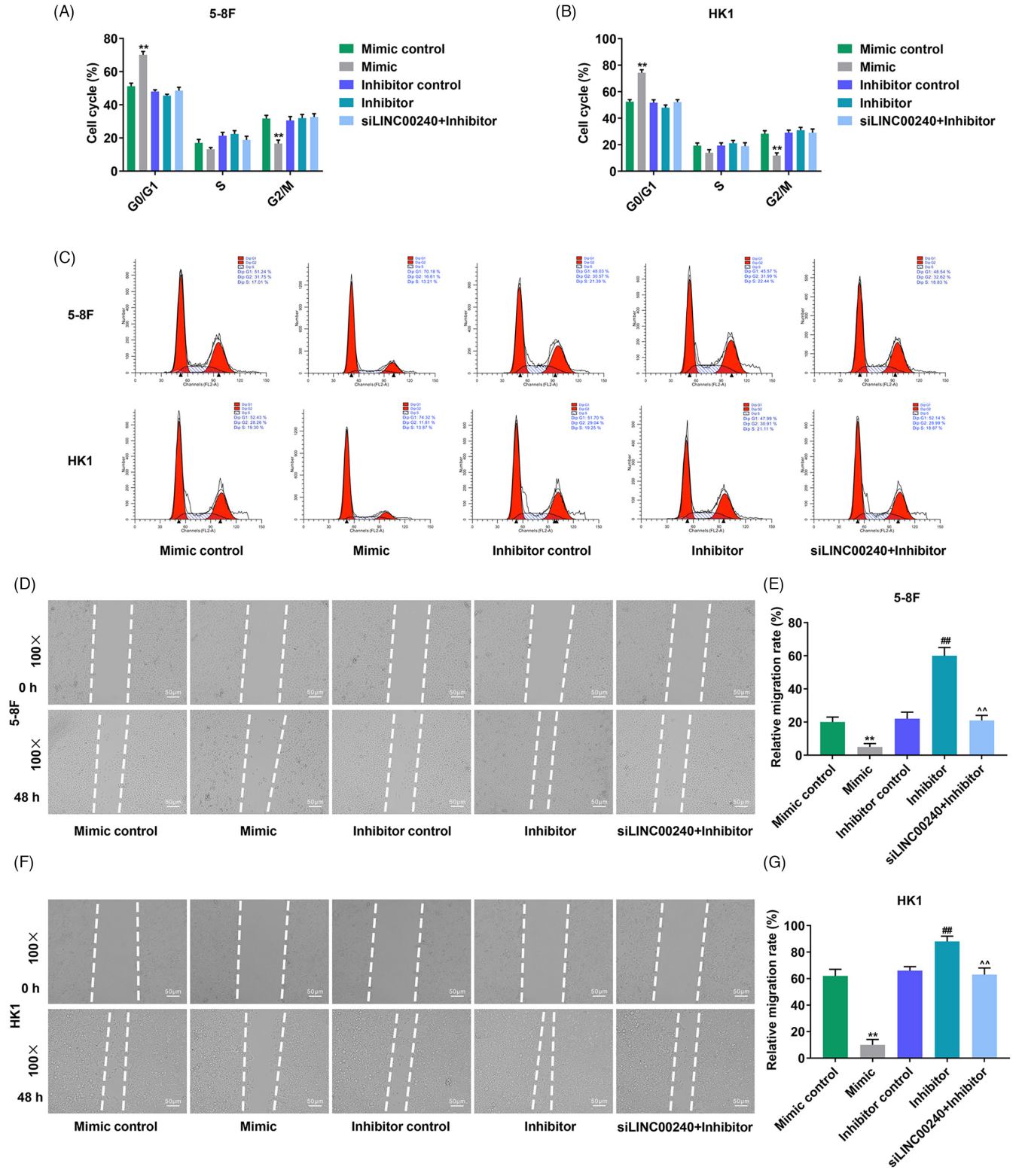

FIGURE 6 The effects of LINC00240 knockdown on cell cycle and migration of NPC cells were achieved by upregulating miR-26a-5p. (A–C) Cell cycle was measured by flow cytometry. (D–G) Cell migration was detected by wound healing assay. $^{**}p < 0.01$ versus mimic control group; $^{\#\#}p < 0.01$ versus inhibitor control group; $^{\wedge\wedge}p < 0.01$ versus inhibitor group. All experiments were repeated independently at least three times. Data are presented as mean ± standard deviation. NPC, nasopharyngeal carcinoma

prognosis of breast cancer patients, has been reported to suppress RNF6 so as to block breast cancer cell growth.[32] Moreover, a previous paper has illustrated that miR-26a-5p acts as a tumor suppressor in NPC.[33] Similarly, in our research, with the establishment of loss- and gain-of-function as well as rescue experiments through transfection of siLINC00240, miR-26a-5p inhibitor, and miR-26a-5p mimic in cells,

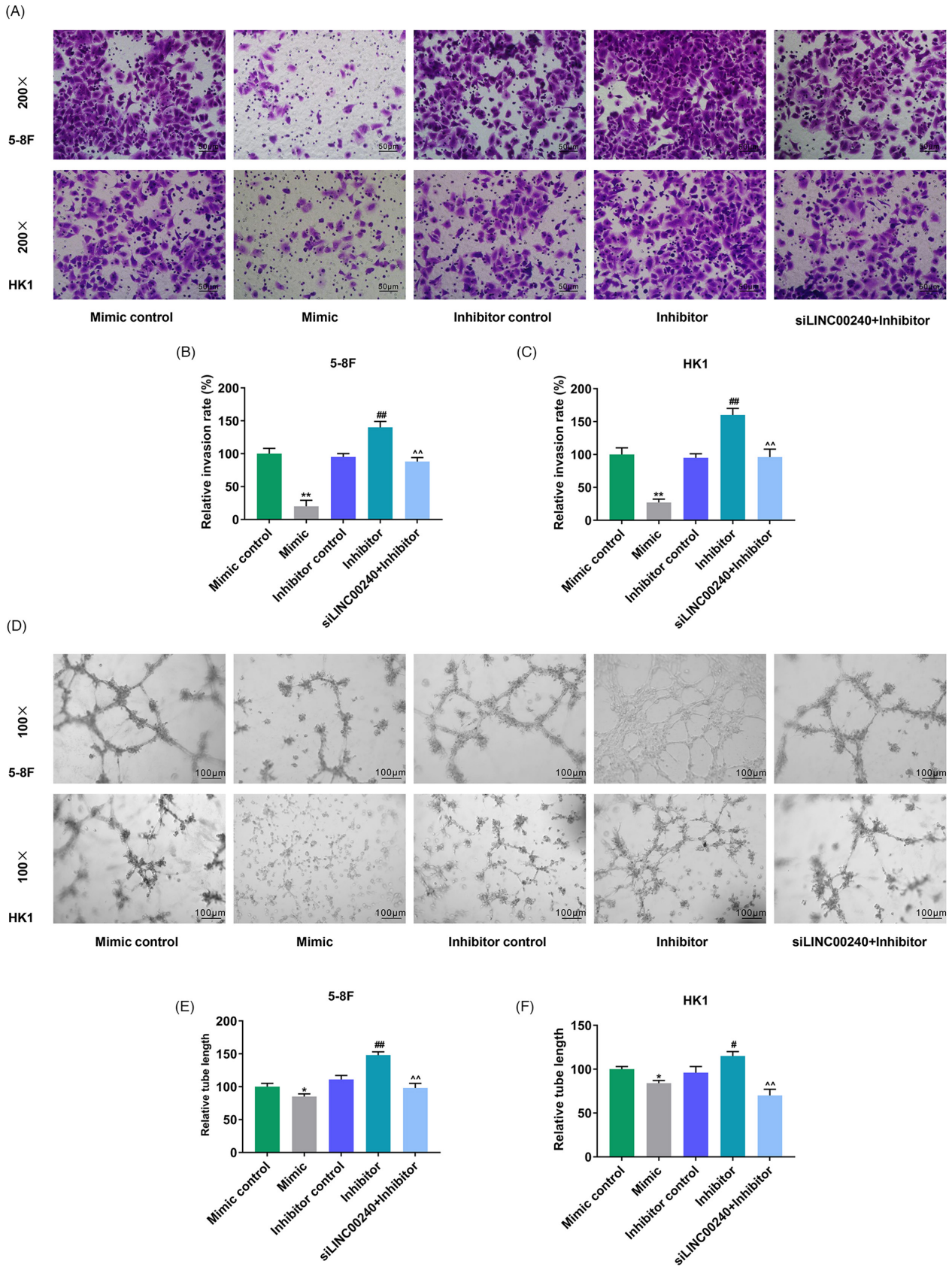

FIGURE 7 The effects of LINC00240 knockdown on invasion and angiogenesis of NPC cells were achieved by upregulating miR-26a-5p. (A–C) Cell invasion was detected by Transwell assay. (D–F) In vitro angiogenesis experiment was used to detect the angiogenesis. $^{*}p < 0.05$, $^{**}p < 0.01$ versus mimic control group; $^{\#}p < 0.05$, $^{\#\#}p < 0.01$ versus inhibitor control group; $^{\wedge\wedge}p < 0.01$ versus inhibitor group. All experiments were repeated independently at least three times. Data are presented as mean ± standard deviation. NPC, nasopharyngeal carcinoma

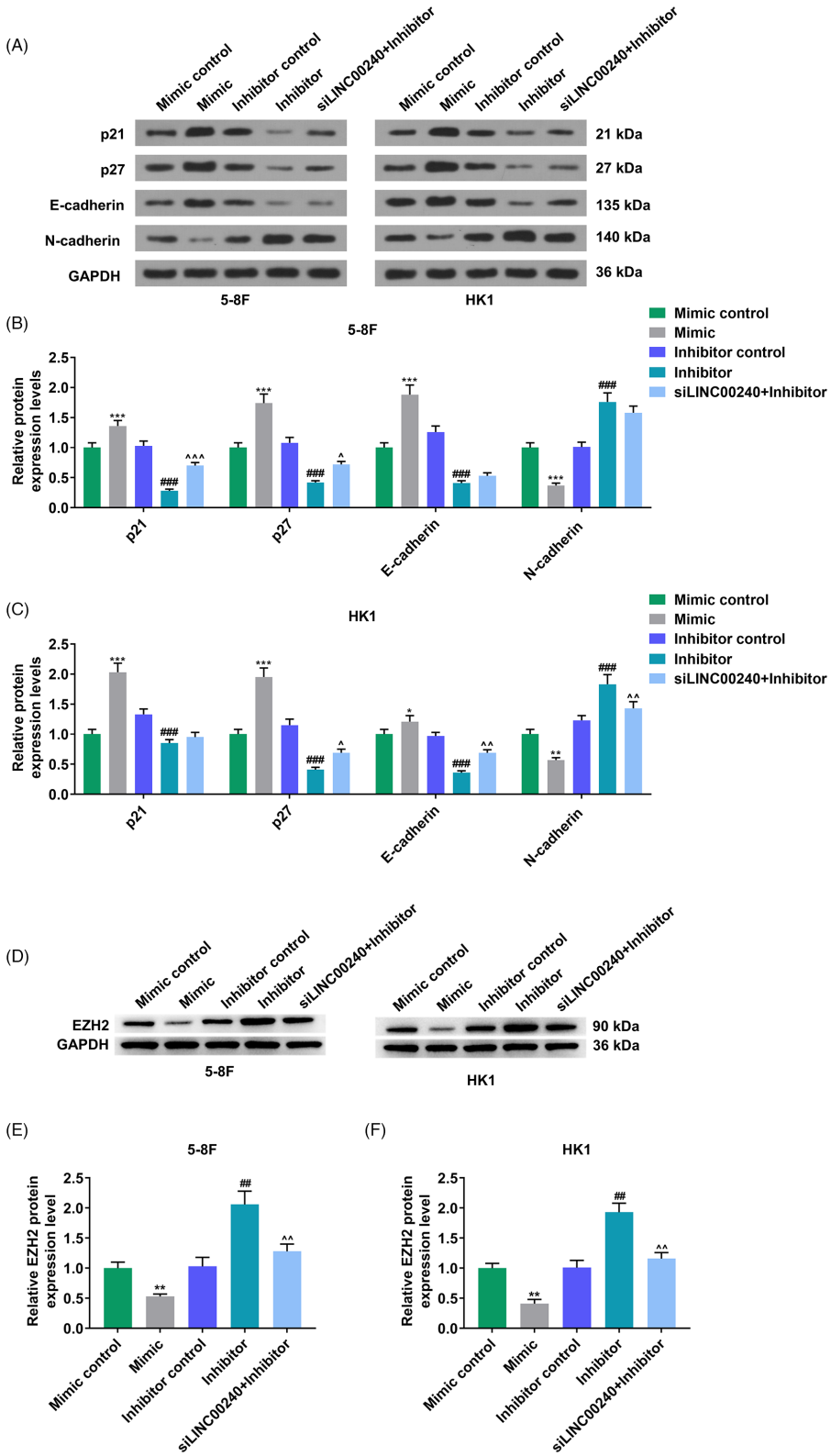

FIGURE 8 MiR-26a-5p inhibitor upregulated N-cadherin and EZH2 protein expression and inhibited p21, p27 and E-cadherin expression in NPC cells, while LINC00240 knockdown reversed its effect. (A–C) The cell cycle (p21, p27) and epithelial-mesenchymal transition (EMT)-related proteins (E-cadherin and N-cadherin) expression of 5-8F and HK1 cells was detected by Western blot. GAPDH was the loading control. (D–F) EZH2 protein expression of 5-8F and HK1 cells was detected by Western blot. GAPDH was the loading control. $^{*}p < 0.05$, $^{**}p < 0.01$, $^{***}p < 0.001$ vesrus mimic control group; $^{\#\#}p < 0.01$, $^{\#\#\#}p < 0.001$ versus inhibitor control group; $^{\wedge}p < 0.05$, $^{\wedge\wedge}p < 0.01$, $^{\wedge\wedge\wedge}p < 0.001$ versus inhibitor group. All experiments were repeated independently at least three times. Data are presented as mean ± standard deviation. EZH2, enhancer of zeste 2 polycomb repressive complex 2 subunit; GAPDH, glyceraldehyde-3-phosphate dehydrogenase; NPC, nasopharyngeal carcinoma

we discovered that the miR-26a-5p mimic repressed NPC cell proliferation, invasion, migration, and angiogenesis, while it facilitated apoptosis, whereas the miR-26a-5p inhibition advanced cell proliferation, invasion, migration, as well as angiogenesis, while it inhibited apoptosis, and LINC00240 knockdown partially reversed the effects of miR-26a-5p inhibitor in those aspects above. In addition, consistent with the studies about miR-26a in NPC,[18,19] the consequences of Western blot presented that miR-26a-5p upregulation inhibited EZH2 and its downregulation advanced EZH2, whereas the knockdown of LINC00240 partly offset the EZH2 increase mediated by miR-26a-5p downregulation. EZH2 is highly expressed and realized a positive effect on the progress of multiple malignancies, the participation of which in NPC has been verified in several reports.[18,19] Those findings suggested that LINC00240 knockdown repressed cell proliferation, invasion, migration, and angiogenesis, while it facilitated apoptosis via negatively regulating miR-26a-5p in NPC through inhibition of EZH2.

5 | CONCLUSIONS

To sum up, this study reveals that LINC00240 knockdown suppressed NPC progression by targeting miR-26a-5p through inhibiting EZH2, which implied that it was a promising target for NPC treatment. Future researches will focus on in vivo experiments to verify the feasibility of the results acquired in this work.

ACKNOWLEDGEMENT

Not applicable.

CONFLICT OF INTEREST

The authors declare no conflicts of interest.

AUTHOR CONTRIBUTIONS

Substantial contributions to conception and design, and rafting the manuscript or critically revising it for important intellectual content: X. Chen. Data acquisition, data analysis, and interpretation: G.X. Wu, J. Qing, C.L. Li, X.D. Chen, and J. Shen. Final approval of the version to be published: All authors. All authors agree to be accountable for all aspects of the work in ensuring that questions related to the accuracy or integrity of the work are appropriately investigated and resolved.

DATA AVAILABILITY STATEMENT

The analyzed datasets generated during the study are available from the corresponding author on reasonable request.

ORCID

Jian Shen https://orcid.org/0000-0002-9283-2984

REFERENCES

1. Chua MLK, Wee JTS, Hui EP, Chan ATC. Nasopharyngeal carcinoma. *Lancet*. 2016;387(10022):1012-1024.
2. Perri F, Della Vittoria Scarpati G, Caponigro F, et al. Management of recurrent nasopharyngeal carcinoma: current perspectives. *Onco Targets Ther*. 2019;12:1583-1591.
3. Wee JT, Soong YL, Poh SS, Chua ML. Nasopharyngeal carcinoma-some closing remarks. *Chin Clin Oncol*. 2016;5(2):29.
4. Pan JJ, Ng WT, Zong JF, et al. Proposal for the 8th edition of the AJCC/UICC staging system for nasopharyngeal cancer in the era of intensity-modulated radiotherapy. *Cancer*. 2016;122(4):546-558.
5. Morris LG, Chan TA. Therapeutic targeting of tumor suppressor genes. *Cancer*. 2015;121(9):1357-1368.
6. Ling H, Fabbri M, Calin GA. MicroRNAs and other non-coding RNAs as targets for anticancer drug development. *Nat Rev Drug Discovery*. 2013;12(11):847-865.
7. Reynolds MM, Veverka KK, Gertz MA, et al. Reply. *Am J Ophthalmol*. 2018;186:170.
8. Liu Y, Liu DW. [Long non-coding RNA and wound healing]. *Zhonghua Shao Shang Za Zhi*. 2016;32(12):735-739.
9. Bhan A, Mandal SS. LncRNA HOTAIR: a master regulator of chromatin dynamics and cancer. *Biochem Biophys Acta*. 2015;1856(1):151-164.
10. Ma X, Zhang B, Zheng W. Genetic variants associated with colorectal cancer risk: comprehensive research synopsis, meta-analysis, and epidemiological evidence. *Gut*. 2014;63(2):326-336.
11. Isin M, Uysaler E, Ozgur E, et al. Exosomal lncRNA-p21 levels may help to distinguish prostate cancer from benign disease. *Front Genet*. 2015;6:168.
12. Yang S, Ning Q, Zhang G, Sun H, Wang Z, Li Y. Construction of differential mRNA-lncRNA crosstalk networks based on ceRNA hypothesis uncover key roles of lncRNAs implicated in esophageal squamous cell carcinoma. *Oncotarget*. 2016;7(52):85728-85740.
13. Li Y, Yan J, Wang Y, Wang C, Zhang C, Li G. LINC00240 promotes gastric cancer cell proliferation, migration and EMT via the miR-124-3p / DNMT3B axis. *Cell Biochem Funct*. 2020;38(8):1079-1088.
14. Bu WJ, Fang Z, Li WL, et al. LINC00240 sponges miR-4465 to promote proliferation, migration, and invasion of hepatocellular carcinoma cells via HGF/c-MET signaling pathway. *Eur Rev Med Pharmacol Sci*. 2020;24(20):10452-10461.
15. Zhang Y, Li X, Zhang J, Liang H. Natural killer T cell cytotoxic activity in cervical cancer is facilitated by the LINC00240/microRNA-124-3p/STAT3/MICA axis. *Cancer Lett*. 2020;474:63-73.
16. Ballantyne MD, McDonald RA, Baker AH. lncRNA/MicroRNA interactions in the vasculature. *Clin Pharmacol Ther*. 2016;99(5):494-501.
17. Liu B, Pan S, Xiao Y, Liu Q, Xu J, Jia L. LINC01296/miR-26a/GALNT3 axis contributes to colorectal cancer progression by regulating O-glycosylated MUC1 via PI3K/AKT pathway. *J Exp Clin Cancer Res*. 2018;37(1):316.
18. Lu J, He ML, Wang L, et al. MiR-26a inhibits cell growth and tumorigenesis of nasopharyngeal carcinoma through repression of EZH2. *Can Res*. 2011;71(1):225-233.
19. Yu L, Lu J, Zhang B, et al. miR-26a inhibits invasion and metastasis of nasopharyngeal cancer by targeting EZH2. *Oncol Lett*. 2013;5(4):1223-1228.
20. Urabe F, Kosaka N, Sawa Y, et al. miR-26a regulates extracellular vesicle secretion from prostate cancer cells via targeting SHC4, PFDN4, and CHORDC1. *Sci Adv*. 2020;6(18):eaay3051.
21. Livak KJ, Schmittgen TD. Analysis of relative gene expression data using real-time quantitative PCR and the 2(-Delta Delta C(T)) Method. *Methods*. 2001;25(4):402-408.
22. Dykes IM, Emanueli C. Transcriptional and post-transcriptional gene regulation by long non-coding RNA. *Genomics Proteomics Bioinformatics*. 2017;15(3):177-186.
23. Engreitz JM, Pandya-Jones A, McDonel P, et al. The Xist lncRNA exploits three-dimensional genome architecture to spread across the X chromosome. *Science*. 2013;341(6147):1237973.
24. Kazemzadeh M, Safaralizadeh R, Orang AV. LncRNAs: emerging players in gene regulation and disease pathogenesis. *J Genet*. 2015;94(4):771-784.

25. Ma DD, Yuan LL, Lin LQ. LncRNA HOTAIR contributes to the tumorigenesis of nasopharyngeal carcinoma via up-regulating FASN. *Eur Rev Med Pharmacol Sci*. 2017;21(22):5143-5152.
26. Wang YJ, Zhang HQ, Han HL, Zou YY, Gao QL, Yang GT. Taxifolin enhances osteogenic differentiation of human bone marrow mesenchymal stem cells partially via NF-kappaB pathway. *Biochem Biophys Res Comm*. 2017;490(1):36-43.
27. Hu X, Jiang H, Jiang X. Downregulation of lncRNA ANRIL inhibits proliferation, induces apoptosis, and enhances radiosensitivity in nasopharyngeal carcinoma cells through regulating miR-125a. *Cancer Biol Ther*. 2017;18(5):331-338.
28. Ku GW, Kang Y, Yu SL, et al. LncRNA LINC00240 suppresses invasion and migration in non-small cell lung cancer by sponging miR-7-5p. *BMC Cancer*. 2021;21(1):44.
29. Li HH, Wang JD, Wang W, Wang HF, Lv JQ. Effect of miR-26a-5p on gastric cancer cell proliferation, migration and invasion by targeting COL10A1. *Eur Rev Med Pharmacol Sci*. 2020;24(3):1186-1194.
30. Wu K, Mu XY, Jiang JT, et al. miRNA-26a-5p and miR-26b-5p inhibit the proliferation of bladder cancer cells by regulating PDCD10. *Oncol Rep*. 2018;40(6):3523-3532.
31. Ye MF, Lin D, Li WJ, Xu HP, Zhang J. MiR-26a-5p serves as an oncogenic microrna in non-small cell lung cancer by targeting FAF1. *Cancer Manag Res*. 2020;12:7131-7142.
32. Huang ZM, Ge HF, Yang CC, et al. MicroRNA-26a-5p inhibits breast cancer cell growth by suppressing RNF6 expression. *Kaohsiung J Med Sci*. 2019;35(8):467-473.
33. Yin X, Gu X, Li F, Ye F, Liu F, Wang W. LncRNA SNHG6 accelerates nasopharyngeal carcinoma progression via modulating miR-26a-5p/ARPP19 axis. *Bioorg Med Chem Lett*. 2021;40:127955.

How to cite this article: Chen X, Wu G, Qing J, Li C, Chen X, Shen J. LINC00240 knockdown inhibits nasopharyngeal carcinoma progress by targeting miR-26a-5p. *J Clin Lab Anal*. 2022;36:e24424. doi:10.1002/jcla.24424